TRANSACTIONS OF THE INSTITUTE OF FLUID-FLOW MACHINERY

No. 134, 2016, 89–107

Artur Szymański*, Sławomir Dykas, Mirosław Majkut, Michał Strozik

The assessment of the calculation method for determining characteristics of one straight fin labyrinth seal

Silesian University of Technology, Institute of Power Engineering and Turbomachinery, Konarskiego 20, 44-100 Gliwice, Poland

Abstract

The method for the selection of a calculation scheme for the evaluation of the flow behaviour of labyrinth seal with one straight fin, against smooth wall, was presented. Experimental results were obtained from measurement data carried out on the in house, vacuum test section. The advantage of the test rig is a circular shape of the labyrinth specimen, providing similar shape to configuration operated in practise. In computational fluid dynamics study different types of mesh resolution were tested, with variable volume discretization in the area of a labyrinth fin tip. Moreover, a wide range of turbulence models basing on k-ε and k-ω, exploiting the (Reynolds Average Navier Stokes) scheme, for the flow pattern evaluation, were examined. All obtained results were compared with literature data, covering research conducted on similar configurations. The presented study shows challenges as well as the possibilities of calculation simplification and compares results obtained by means of simulations and experiment. The proposed method is characterised by excellent agreement of computational results with experiment data.

Keywords: Labyrinth seals; Computational Flow Dynamics (CFD); Seal; Smooth; Turbomachinery; Leakage flow rate

Nomenclature

A	–	flow area, m^2
b	–	labyrinth fin tip width, m
c	–	velocity, m/s
C_D	–	discharge coefficient
h	–	labyrinth fin height, m

*Corresponding Author. Email adress: artur.szymanski@polsl.pl

$\dot{m}$ – mass flow rate , kg/s
R – gas constant, for air $R = 287.05$ Jkg^{-1}K^{-1}
s – clearance, m
T – temperature, K
u – tangential velocity, m/s
x – axial distance, m

Greek symbols

π – pressure ratio
κ – specific heat ratio, for air $\kappa = 1.4$
Ψ – flow function

Subscripts

0 – total parameter
ax – axial
id – ideal
s – static

1 Introduction

New requirements imposed on aircraft and stationary gas turbines manufacturers assumes reduced emission of pollutants and improved reliability, safety and comfort of the operation. The essential for an improvement in energy conversion efficiency in gas turbines was noticed already in the 1950's. Since that time, more than a 50% drop in fuel consumption per unit may be observed in state-of-the art machines compared to engines constructed in the 1940's [1]. One of the methods of improving machine efficiency is to optimize gas turbine sealing operating conditions. Type of applied sealing has an impact not only on the size of leakage but also on dynamic behaviour of rotor and entire engine fuel consumption, the temperature distribution downstream the stage, power decrease of engine, as well as the risk of creep phenomenon. The results of investigation presented in [2] may be an example here. They indicate that a rise in the leakage through the gas turbine stage sealing from 3% to 4.5% of main mass flow (a relative 50% rise), involves an increase in the turbine outlet temperature by 15 °C. This in turn decreases durability by approximately 30% due to the risk of creep occurrence [2]. Leakage losses in turbomachinery are one of the most significant loss components. They comprise the entirety of leakage due to the pressure distribution in the machine (compressor or turbine). Flowing through a leaky section, the medium does not do useful work. Moreover, it becomes a source of additional losses related to mixing with the main flow with different parameters. The mixing of the mediums also involves disturbance in the flow field, which is a source of losses in following blade stages. The key to effective and safe operation of turbomachinery is to

maintain appropriate clearances between stationary and rotating elements. The bigger the clearance between elements operating in different pressure areas, the higher the leakage and, consequently, the lower the efficiency. The leakage also affects the streamline shape and the pressure distribution in the next stage. In aircraft turbines there are more than 50 places that need sealing, but the most essential seals are used:

- in places where the shaft extends beyond the casing,
- on tips of axial stages – clearance between the shrouding and the casing,
- between the shaft and the stator disc – in the case of impulse turbines with discs,
- between the shaft and the stator blade bottom – in the case of reaction turbines with drums,
- between the shaft and the compressor last stage outlet (compressor discharge pressure sealing).

The whole range of different kinds of sealing are applied in turbomachinery. Labyrinth seals are a non-contacting type of sealing. Due to their very simple design they are the most common turbomachinery sealing type. However, the leakage is big compared to other design approach. Therefore, they are used due to a number of advantages. Structurally, they are made of a few rings, creating a series of annular cavities. They are used not only in turbines but also in pumps, fans, compressors, and bearings. They consist of 1 to even 15 fins. Experimental research related to the flow through the turbine seals is taken up by few research centres. Most experiments focus on stationary models, where the motion of the labyrinth structure relative to the casing is omitted. The conducted experiments proved that such simplification is correct if the flow velocity over the labyrinth seal fin is higher than the rotor tangential velocity – in this case stationary test rigs map the flow behaviour correctly and the condition $u/c_{ax} < 1$ is satisfied [3,4]. Nonetheless, when circumferential velocity is higher than the axial component, the condition $u/c_{ax} < 1$ is not met and a mass flow rate drop comparing to the stationary model occurs. In papers [3,4] also was mentioned that the mass flow through the seal depends on many parameters, such as the total inlet pressure, the total inlet temperature, the inlet Reynolds number, the angle of inflow onto the seal (initial preswirl), the pressure ratio, the seal relative motion and the structure of the seal. In experiments presented in [5–7] the observed parameters were the discharge coefficient, and the pressure and temperature distribution along the seal structure. These parameters allowed the determination of the loss coefficient distribution. In presented works two types of the feeding system were used – pressurized and vacuum. In all cases the authors emphasize the importance of the

measurement of the clearance size as the parameter with the biggest impact on the measuring uncertainty. Experimental work presented in [4], shows detailed in study of real conditions of the seal operation, like in an engine turbine. In the study, a vacuum feeding system with air with ambient temperature at a non-rotating axial architecture of the labyrinth seal was used. The air was sucked by the vacuum installation through the test rig into a vacuum vessel where the constant pressure value prevails. The investigated structure maintains all dimensions of fins, clearances, and angles the same as in real operating machines. The paper presents the challenges in experimental testing performed on an in-house nonrotating test rig of the Institute of Power Engineering and Turbomachinery (IPET) of the Silesian University of Technology (SUT). The aim of this study was to assess the calculation method for one fin labyrinth seal behaviour, comparing the results with in-house measurement data, as well as with data available in the literature.

2 Vacuum installation

For the purpose of experimental research, the vacuum air installation was deployed. The installation consists of a Roots air blower with the maximum output of 0.2 kg/s (10 Nm^3/s) with operating pressure providing critical pressure ratios, a $3m^3$ pressure vessel and aluminium pipeline system connecting all the components together (Fig. 1). The total volume of pipeline system and pressure vessel is about 3.5 m^3, which is large when compared to the expected flow rates. This capacity dumps pressure fluctuation well, providing stable pressure distributions at the test rig outlet. The diameter of the pipelines is DN100, which ensures low velocity and pressure losses. The test rig is described in following subsections. Figure 1 presents a simplified diagram of the installation. The air is sucked from surrounding through 4 m long pipe, which makes it possible to create appropriate conditions for the mass flow measurement upstream of the test rig, and flows into the test section equipped with the measuring system. The mass flow measurement is located at the inlet pipe, 3 m downstream of the pipe inlet. The inlet total pressure and total temperature is also evaluated. Then air flows into the pressure vessel. On the other side, secondary air is sucked in from the surroundings through DN50 throttling valve – allowing to regulate pressure inside the vessel. All valves are controlled by an electric actuator, which allows a precise and repeatable setting of the opening angle which is remote-adjusted from the measuring system. Finally air flows through the Roots air blower, and after that into the environment.

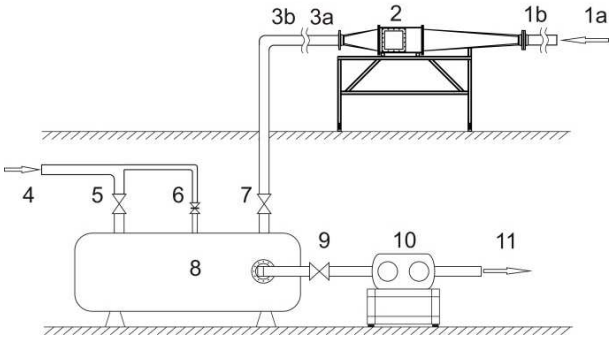

Figure 1: Experimental installation intended for the turbine seal testing in the IPET of the SUT. Installation description: 1 – test rig inlet (total parameters (1a), mass flow (1b) measurement), 2 – test rig with measurement system, 3a and 3b – mass flow measurement, 4 – secondary air inlet, 5 – cut-off valve, 6 – remote controlled valve, 7 – cut-off valve, 8 – 3 m^3 vessel, 9 – cut-off valve, 10 – roots air blower, 11 – outlet.

3 Test rig

In order to perform experimental study, the SUT developed in-house test rig has been used. The test section was fed with previously described vacuum installation, thereby forcing the flow through the sealing specimen. The main feature of the test rig was unusual approach design. The body of the test section is made from thick-walled welded tube (Fig. 2), wherein the circular samples of labyrinth seals are placed. The test section body is made of high quality structural steel. Labyrinth seals models are made of duralumin PA9 characterized by good machinability. Selected materials due to its parameters, allowed for a very precise manufacturing process. The proposed approach significantly simplifies the measurement process, reducing installation and sealing time to a minimum. The described test rig does not require setting the clearance, and adjusting the position of the seal fins. The gap between the tip of the tooth and the housing is a result of geometrical dimensions of the components. However, the presented design approach requires very precise machining of components, taking into account a very accurate alignment of the entire structure. The as-built measurements of elements showed the manufacturing accuracy within a 0.01 mm range. Pressure taps for measuring static pressure behind the seal are placed peripherally every 120°. This measurement was used to determine the pressure ratio needed to determine the performance characteristics of the structure. Despite its simple design, this test rig allows for reliable and very repeatable measurement. The main drawback of the presented test stand is a lack of possibility for measurements of different

labyrinth seal facings – like honeycomb. Only smooth land is available. Details of investigated geometry, applied both in experimental and computational fluid dynamics (CFD) approach, are shown in Fig. 4.

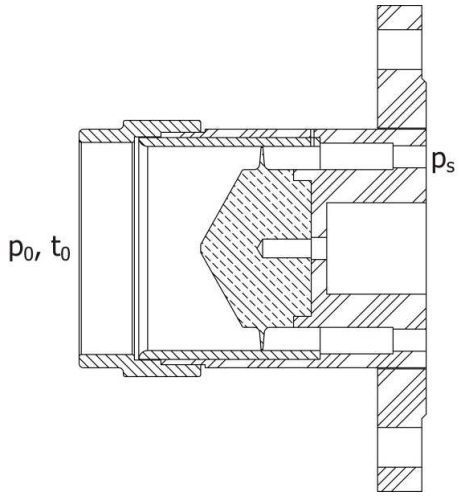

Figure 2: Cross section of circular test rig, where p_0 is the total pressure, t_0 is the total temperature and p_s is static pressure.

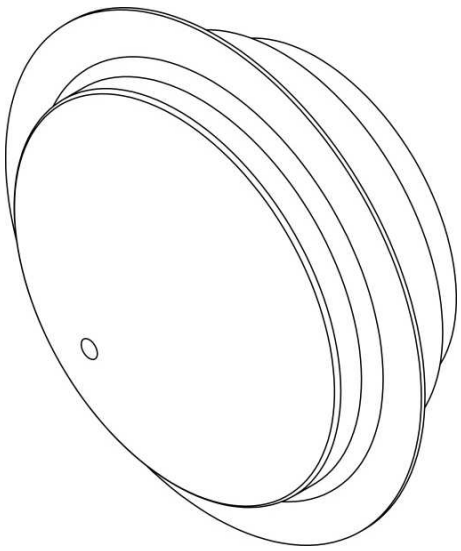

Figure 3: Circular labyrinth specimen.

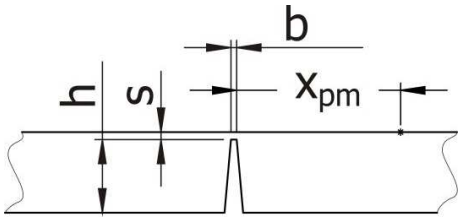

Figure 4: Labyrinth seal dimensions: h – height of the seal tooth, s – gap between the tooth tip and the housing, b – width of the tooth tip, x_{pm} – axial distance between the fin edge and the place of static pressure measurement (defining the operational pressure ratio π). Dimension value: $h = 10$ mm, $s = 0.5$–1.5 mm, $b = 0.8$ mm, $x_{pm} = 22.4$ mm.

It is worth mentioning that in the CFD evaluation method, pressure ratio was evaluated in the same way.

4 Results evaluation

To evaluate results, algorithm presented below was applied. In this study dimensionless flow parameters – discharge coefficient and flow function versus operational pressure ratio were used. This approach was applied both for experimental and computational studies. Static pressure measurement, which is used for the evaluation of the operating pressure ratio, was set behind the fin. The pressure ratio is defined as the quotient of the inlet total pressure, p_{0in}, and static pressure, p_s, measured in the presented point

$$\pi = \frac{p_{0in}}{p_s} \,. \tag{1}$$

Analysing the possibility of limiting the leakage through the tested structure of the seal, pretty soon it turns out that the value of the mass flow rate as an indicator for the evaluation and comparison is insufficient. It depends not only on the architecture of the seal itself, but also on the total inlet parameters, which – due to the characteristic of the installation – are variable in time. Therefore frequently cited in the literature dimensionless flow coefficients are used [4]. These allow for comparison of the leakage through the different structures of different shapes and sizes by varying values of fluid parameters. The first is discharge coefficient, C_D, defined as a ratio of the mass flow rate, $\dot{m}$, through the model of the seal to that of an isentropic nozzle with the same surface area, $\dot{m}_{id}$,

$$C_D = \frac{\dot{m}}{\dot{m}_{id}} \,. \tag{2}$$

The mass flow rate under perfect fluid condition is defined as

$$\dot{m}_{id} = \frac{p_{0\text{in}} A}{\sqrt{T_{0\text{in}}}} \sqrt{\frac{2\kappa}{R(\kappa-1)} \left[\left(\frac{1}{\pi}\right)^{2/\kappa} - \left(\frac{1}{\pi}\right)^{(\kappa+1)/\kappa} \right]} \,. \tag{3}$$

Moreover, there is another flow function parameter, Ψ, which is defined as

$$\Psi = \frac{\dot{m}\sqrt{T_{0in}}}{A\, P_{0in}} \,. \tag{4}$$

5 Validation of the calculation model for the circular shape of the labyrinth seal

Currently, ongoing development in the field of computer technology allows us, to perform complex calculations once impossible. CFD methods can be applied as a

fairly quick way to evaluate the flow field in the analyzed area, accelerating the design or optimization of different structures in terms of flow [8]. Unfortunately, the great multitude of turbulence models, the geometrical or calculation model parameters results in possibility of making a mistake. Due to this fact, the best way for proper calculation method selection is to support it with experimental research. For this purpose, this section presents an approach for selection of the calculation method for determination of the flow field in a circular shape labyrinth seal specimen. For this purpose commercial software Ansys CFX 16.2 [15] was employed. The calculation process was divided into the following stages.

- analysis of the possibilities to simplify the geometry of the inlet chamber in the 2D model,
- analysis of the possibilities to simplify the 3D geometry in the circumferential direction [8],
- the selection of method for spatial discretization of the 2D calculation model, with different turbulence models,
- comparison of experimental data with the CFD results.

The aim of the calculations as well as the measurement was to determine the dimensionless flow rate, C_D, which is a measure of the sealing efficiency. This parameter depends on a number of parameters, and often due to unsteady nature of the flow phenomenon, fluctuates during the measurement or calculation. Therefore, the discharge coefficient was determined for the parameters measured in about 90 s. When calculations are considered, there is also required a considerable accuracy, providing a constant value of flow field. For this purpose, it was established that the parameter terminating calculation is the difference between the mass flow rate evaluated on the boundary conditions – inlet and outlet. Maintaining the mass imbalance parameter for following 100 iterations below 0.01% resulted in fluctuations of the C_D parameter lower than 0.001. This approach guaranteed numerically independent result, uninterrupted by mathematically generated unsteady flow phenomena. The place of measurement of the static pressure for the purpose of determining pressure ratio, π, is shown in Fig. 2. It corresponds to the place where the static pressure was measured at the test rig. All presented calculations were performed in a steady-state scheme.

6 Computational approach for the 2D model

The use of two-dimensional computational model is preferred in many cases because it provides valuable information about the flow field, keeping relatively short time of calculation, resulting from the significantly reduced number of grid nodes, and the skipping of one direction in the numerical model. Ansys CFX software itself does not give the direct possibility of performing two-dimensional calculations. However, an appropriately selected grid with two elements in one direction – direction to 'eliminate', with the symmetry boundary condition, allows us to perform calculations in a 2D mode [9]. The studied geometries and location of the boundary conditions are illustrated in Figs. 5 and 6. Clearance size for the purpose of numerical approach study was assumed as $s = 1$ mm.

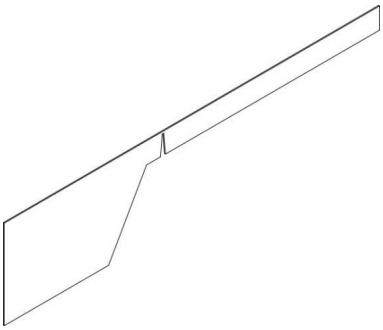

Figure 5: Planar fluid domain of test rig.

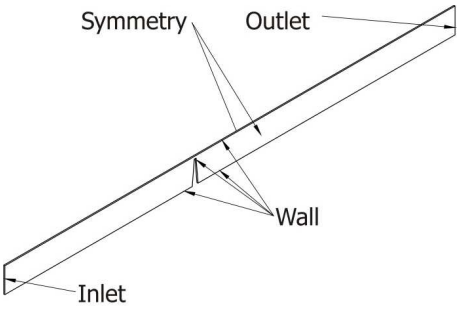

Figure 6: Simplified planar fluid domain, with boundary conditions imposed.

Figure 5 shows the real 2D cross section of flow field through the test section, with angled inlet. For the purpose of simplification of the calculation model, an approach with a straight inlet domain was evaluated. This approach resulted in an average difference in the C_D parameter below 0.4%, and proves that this simplification is fully acceptable. Moreover, the number of grid nodes were reduced about 30%, as well as the required calculation time.

7 Simplification of 3D geometry of the computational model

In CFD studies simplification of the flow field geometry is desirable. It results in shorter calculation time, and more reliable evaluation. Also in this case, the

numerical test was performed, verifying the ability to achieve maximum simplification of the considered domain. In the first step, as mentioned in the previous section, a possibility of the elimination of the inlet shape of the test rig was examined (Figs. 5 and 6). In turn the impact of domain limitation in the circumferential directions was evaluated. A domain of 360° (Fig. 7) was compared to 90° geometry (Fig. 8), with the same discretization scheme both in axial and circumferential direction, and finally to 2D case (Figs. 5 and 6) . The relative difference between the model 360° and 90° was smaller than 0.1% of C_D. The difference between the 90° model and the two-dimensional circular amounted to 0.2% of C_D. For more accurate evaluation, also a 30° span model with very fine mesh in circumferential direction was taken into account, but no significant differences were found. Therefore, it was assumed that the planar two-dimensional model is sufficient to evaluate the phenomenon occurring in the seal. A similar approach is often found in the literature [10], also for honeycomb structures.

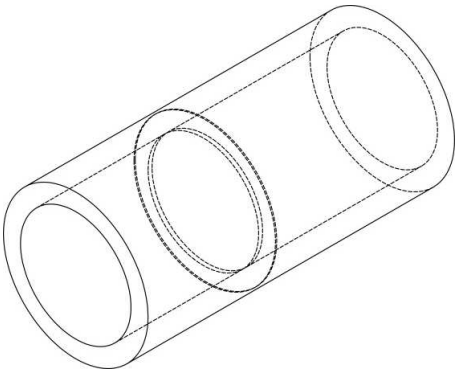

Figure 7: The full 360 degree fluid domain.

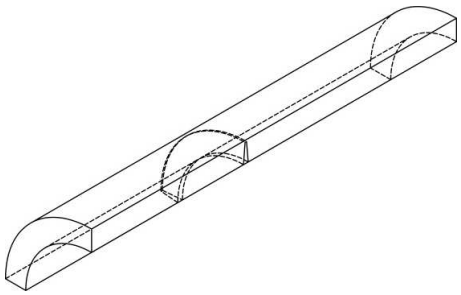

Figure 8: The 90 degree sector of the fluid domain.

8 Mesh and turbulence model study

In the CFD simulations, a proper mesh choice is crucial. Discretisation can have a huge impact on the modeled flow phenomena, as well as on the calculation time. It is very important that the obtained result is dependent on the selected discretization scheme. Accordingly, the presented below calculation tested one case – a 2D labyrinth seal geometry (Fig. 6) with the clearance size $s = 1$ mm. The considered boundary conditions and turbulence models are listed in Tab. 1.

Nine different meshes were applied for each turbulence model (with 44, 88, 183, 282, 440, 636, 972, 2005, and 3500 thousand nodes). It is worth mentioning that mesh sizes were not changed globally, but only in the area above the fin, near walls, and in close region upstream and downstream of the fin.

Table 1: Numerical analysis boundary condition.

Inlet	Total temperature	293 K
	Total pressure	100 kPa
	Turbulence intensity	5%
Outlet	Static pressure	50–95 kPa
	Static pressure profile blend	5%
Global	Working fluid model	Air ideal gas, including Sutherlands viscosity function
	Turbulence models	Steady – state scheme: SST, k-ε, k-ε EARSM, RNG k-ε, BSL, k-Ω
	Heat transfer approach	Total energy, inc. viscous work
	Wall model	Adiabatic, smooth
	Time scale	Automatic, local
	Mass imbalance residual criteria	$< 0.01\%$

The mesh study have shown that with a decrease of the size of grid elements in the area near the tip of the tooth, the mass flow rate as well as the discharge coefficient C_D decreases. In addition, with the increase in the quality of the discretization, results for each model of turbulence standardize in the range of $C_D = 0.66$–0.67. The only exception was the k-ε model, which greatly overestimated results compared to other schemes and the experiment. It is worth mentioning that with the increase of the quality of mesh discretization ($972{\times}10^3$ or greater), models k-ε and k-ε EARSM indicated the lack of desirable imbalance convergence indicating an unstable value of the mass flow (fluctuations of $\pm 3\%$). However, all calculations performed have shown an overestimated value of mass flow, compared to the experiment. The mentioned differences reached up to 4%, except k-ε turbulence model. Basing on this experiment and approach of other scientists [8,11], the SST turbulence model has been selected for further investigation.

The effect of reducing the leakage with the increasing number of mesh nodes can be interpreted by analysing velocity distribution, showing some differences especially in 0–0.4 clearance span (Fig. 10). The place of determination of the velocity distribution is shown in Fig. 9. It also presents the phenomenon of de-

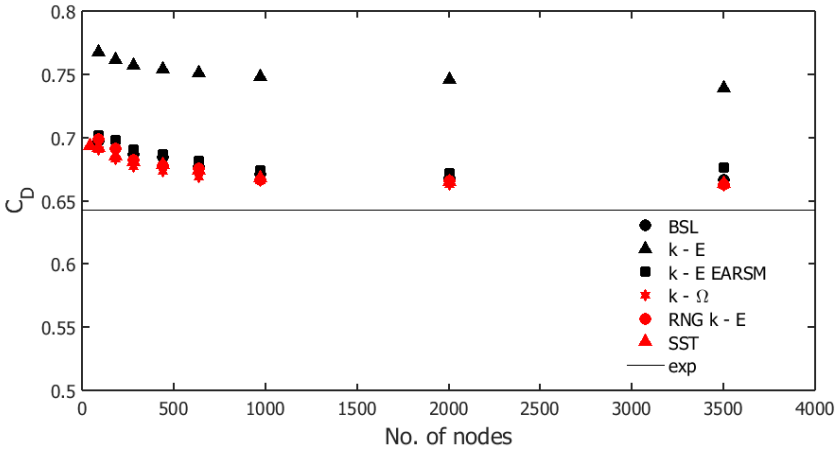

Figure 9: Mesh study for 2D model results.

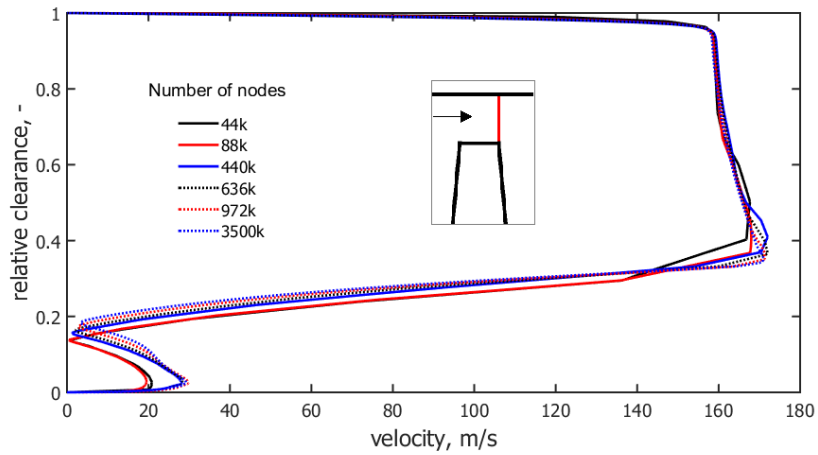

Figure 10: Cross section of circular test rig SST.

tachment of the stream behind the edge of the labyrinth seal, which causes losses and as a result reduces leakage. A higher number of mesh nodes better maps the counter flow vortex appearing at the tip of the fin, resulting in a lower mass flow rate. This example shows how sensitive is featured case. Coarse grids (44, 88 thousand nodes) resulted in different velocity distribution in the specified section, which had a subsequent impact on the global value of the flow rate. Basing on the mesh study, finally method of discretization of 972 thousand nodes has

been selected as the satisfactory one. It is a compromise between the time of calculation and the accuracy. The relative difference between the mesh of 3500 thousand nodes resulting from better flow evaluation is maximum 0.5%, which is satisfactory for further considerations. The way of discretization adopted on the basis of this study has been chosen for further calculations, taking into account different labyrinth seal structures.

Details of selected meshes are presented in Figs. 11 and 12 (Tab. 2). The figures show differences between coarse mesh, and fine mesh – adopted for further calculations. The maximum y^+ parameter in the selected grid is kept below 1, which is satisfactory for a proper wall layer resolution.

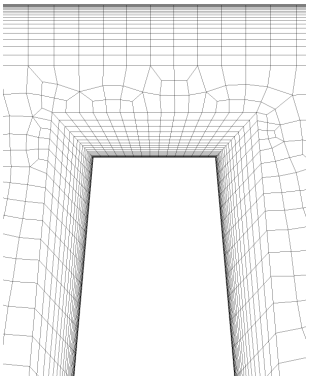

Figure 11: A view of the mesh for 44×10^3.

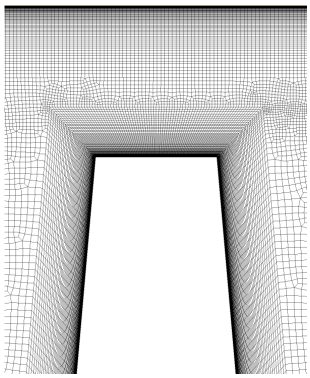

Figure 12: A view of the mesh for 972×10^3 mesh.

Table 2: y^+ vs mesh size

no of nodes	Max y+
44k	6.4
88k	1.6
636k	1.1
972k	*0.9*
3500k	0.6

9 The k-ε and SST turbulence model differences in flow through labyrinth seal evaluation

Due to significant differences between results obtained basing on k-ε and other turbulence models, further investigation searching for differences in the flow field behavior between results obtained by means SST and k-ε model has been done. In both cases the same mesh has been adopted (972 thousand nodes, Fig. 12). Velocity distribution (Fig. 13), streamlines (Fig. 14) and streamlines above the fin were compared. The k-ε model has not modelled the reverse vortex above the fin, and whirls near the fin foot. The mentioned flow detachment in regions near the sharp edges is a main reason of mass flow drop in flow through the throat. Also, vortex downstream of the clearance has a different shape. Moreover, the

velocity distribution is different – the jet behind the tooth is modelled differently. The SST model shows a smaller expansion angle than k-ε. The overestimation of mass flow rate is significant in the case of k-ε, a similar behaviour has been recently reported by other researchers.

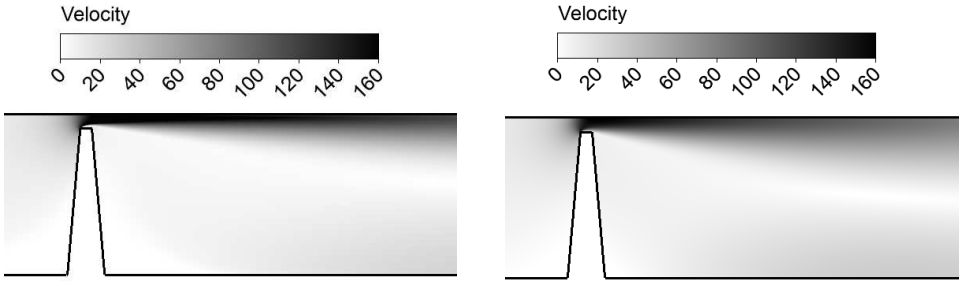

a) b)

Figure 13: Velocity distribution: a) SST turbulence model, b) k-ε.

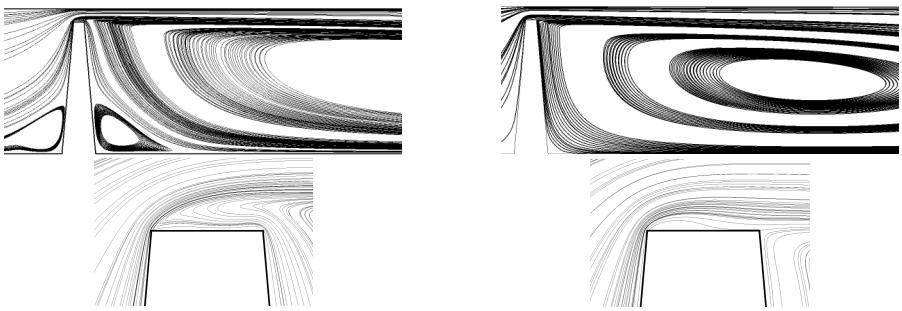

a) b)

Figure 14: Streamlines: a) SST turbulence model, b) k-ε.

In the literature, research of labyrinth seal with one fin has been taken up by few researchers, e.g., Snow [12], Stocker [13]. The limited range of cited investigations, and the fact that they were conducted more than 40 years ago, shows a necessity of verification presented results. Knowledge of the characteristics of C_D values for single fins derived from Snow (1952) can be applied for stepped seals behavior determination, assuming constant pressure loss after every fin. It is furthermore assumed that the pressure ratios are equal for each fin. In addition, it is necessary to use the correction factors depending on the dimensions of the blade and on the pressure ratio [14]. This approach provides accuracy of $\pm 5\%$ for determining the C_D. In studies presented by Snow, flow characteristics of a labyrinth seal with

single tooth as a function of pressure ratio and relative value of the clearance s/b have been analysed. Unfortunately, no details about the geometry or boundary conditions have been presented.

The paper by Stocker [13] exploits measurement performed on labyrinth seals, including a one fin configuration. The presented configuration shows similar parameters as in SUT laboratory ($T_0 = 295$ K, $p_s = 100$ kPa). Some geometrical similarities can be found (Tab. 3). The Stocker geometry is scaled up compared to SUT by factor 2, meeting the same relative clearance. Basing on [11], due to geometry scaling, expected SUT results should be slightly lower than Stocker's.

Table 3: Literature study and SUT geometries.

Parameter	SUT/Stocker	Stocker	SUT
Clearance, s	2–6	0.254	0.5–1.5
Tooth height, H	2	5.08	10
Fin tip thickness, b	3.15	0.254	0.8
Relative clearance, s/b	–	1	0.625–1.875

10 Results

In this section the flow characteristics are presented. Mass flow indicators are described by the previously presented flow function, Ψ, and the discharge coefficient, C_D, as a function of the pressure ratio, π, (Figs. 15–18). Taking into account the results obtained by Stocker, the compatibility of results occurs in the range of low pressure ratio (1–1.3). For pressure rations higher than 1.3 the flow function indicated by Stocker is higher relative to the results obtained by the SUT both in experiment and measurement (Fig. 15). However, it should be noticed that the results were obtained for the same relative size clearance, s/b, while maintaining the geometry scaling factor equal to two (geometry SUT scaled up). A different literature study, done by Braun, determining the impact of scaling on the result indicates the possibility of a difference up to 5% in the case of the scaled geometries.

Results showing the one-fin labyrinth seal behavior (Figs. 16 and 17), indicate similar flow trends obtained both by means of measurement and CFD simulations. At low values of clearance ($s/b < 1$) the differences between the C_D parameter are visible. By high values of the relative clearance ($s/b > 1$), differences between the same clearance size are slight, covering in the range of 0.02 C_D point for both

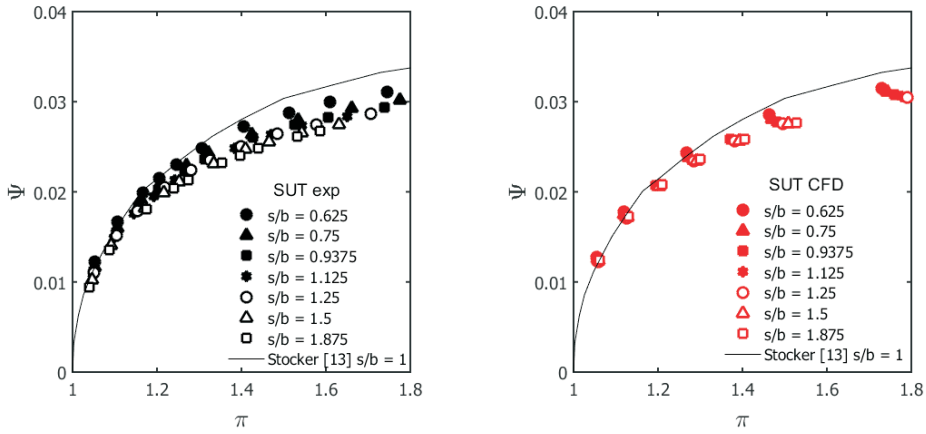

a) b)

Figure 15: Flow function vs. pressure ratio: a) experiment, b) simulation.

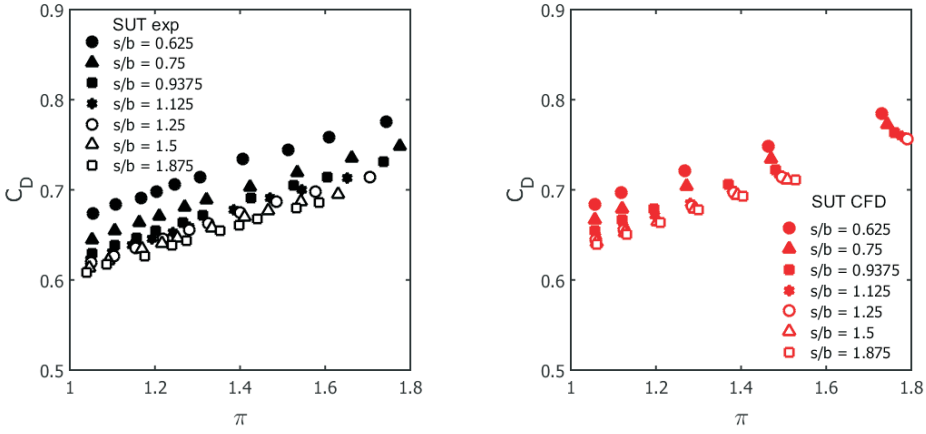

a) b)

Figure 16: Discharge coefficient vs. pressure ratio: a) experiment, b) – simulation.

the calculation and measurement results. The same tendency – drop of the C_D with the rise of clearance was observed for both methods. The results of CFD simulations show a very high agreement with experiment. The average relative error is in the range of 1.5–3.5% of the measured value. What is interesting, a very good agreement was observed for low clearances.

Finally, the obtained results were compared with data delivered by Snow.

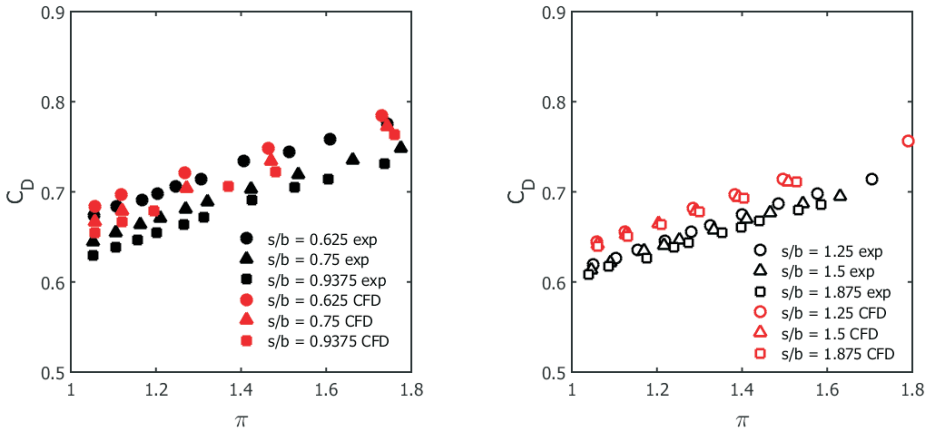

a) b)

Figure 17: Discharge coefficient vs. pressure ratio: a) low relative clearances, b) high relative clearances.

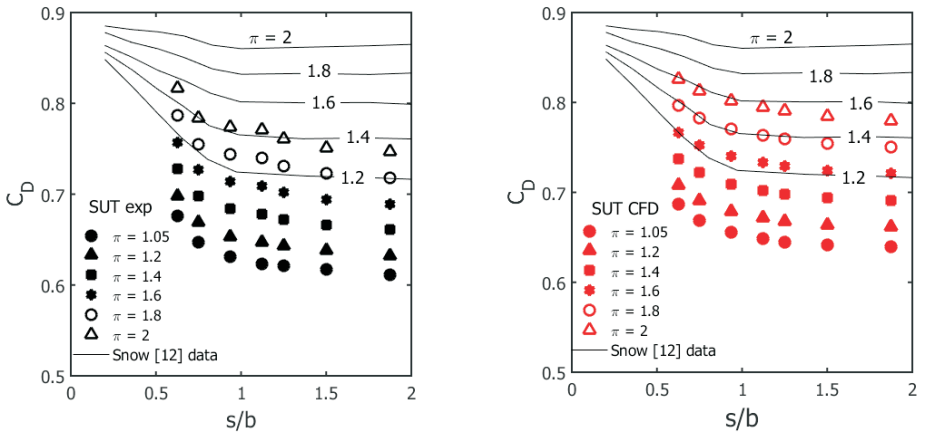

a) b)

Figure 18: Discharge coefficient vs. relative clearance: a) experiment, b) simulation. Snow [12] results included.

Both the measurement data and calculation results show the same tendencies and trends that have been observed by Snow. It indicates a decrease of leakage with increase of relative gap (Fig. 18). Results shown by Snow are overestimated compared to the results obtained by SUT, however taking into account the fact that these studies were conducted in 1950's, one should reflect on their upgrade.

11 Summary

Experimental and computational steady-state approach for determining flow behaviour of one a fin labyrinth seal have been presented. The information about the sealing effectiveness is very important for designing or analysing turbomachinery.

The presented methodology of calculation is sufficient to determine thermodynamic parameters of the gas flowing through the labyrinth seal – flow through narrow cylindrical gaps, and a multitude of geometrical and physical parameters that affect the labyrinth seal flow behaviour. In the literature a number of works on labyrinth seals can be found, but it would be very difficult to create on this basis a certain universal correlation allowing for the determination of the labyrinth seals behaviour. A vast number of geometrical parameters, feeding fluid pressure and temperature cases that result may not be consistent with each other.

The study indicates that the viscosity turbulence models satisfactorily model the flow behaviour in the labyrinth seal, however, tend to overestimate the presented results (2–4%). This is due to the fact of averaging flow parameters in a steady-state mode, without solving unsteady phenomena occurring in the analysed structure. For obtaining better results authors recommend performing calculations in an unsteady scheme, with high resolution of unsteady phenomenon, which may affect the global discharge. However, due to the significant hardware requirements and time needed, steady-state solution is some compromise between the accuracy and duration of the calculations. The presented mesh study reveals the sufficient special discretization, proving acceptable agreement of calculations with experiment. The final mesh consisted of approximately one million geometrical nodes in a quasi 2D approach proposed by Ansys CFX.

Acknowledgment Presented studies were performed thanks to Silesian University of Technology support for young researchers no. 08/050/BKM16/0088.

Received in September 2016

References

[1] Steinetz B.M., Hendricks R.C., Munson J.: *Advanced seal technology role in meeting next generation turbine engine goals*. AC/322(AVT)TP/9RTO, Paper RTO–MP–8, 1999.

[2] Hendricks R.C., Steinz B.M., Braun M.J.: *Turbomachine sealing and secondary flows. Part 1 – Review of sealing performance, customer, engine designer, and research issues*.' NASA/TM—2004-211991/PART1, 2004.

[3] R. Paolio, Moore S., Cloud D., Glahn J.A.: *Impact of rotational speed on the discharge characteristic of stepped labyrinth seals*. Conf.: ASME Turbo Expo 2007, DOI: 10.1115/GT2007-28248, 2007.

[4] Denecke J., Dullenkopf K., Wittig S., Bauer H.: *Experimental investigation of the total temperature increase and swirl development in rotating labyrinth seals*. In: Proc. ASME Turbo Expo 2005 Power for Land, Sea and Air, GT2005-68677, 2005.

[5] Massini D., Facchini B., Micio M., Bianchini C., Ceccherini A., Innocenti L.: *Analysis of flat plate honeycomb seals aerodynamic losses: effects of clearance*. In: 68th Conf. Italian Thermal Machines Engineering Association, ATI2013, Energy Procedia **45**(2014), 502–511.

[6] Doerr L.: *Modellmessungen und Berechnungen zum Durchflussverhalten von Durchblicklabyrinthen unter Berĺucksichtigung der ĺUbertragbarkeit*. PhD thesis, Institut für Thermische Stromungsmaschinen, Universitat Karlsruhe (TH), 1985.

[7] Braun E., Dullenkopf K., Bauer H.J.: *Optimization of labyrinth seal performance combining experimental, numerical and data mining methods*. ASME Paper GT2012-68077, 2012.

[8] Bochon K.: *Numerical investigation of fluid flow and heat transfer phenomena in selected parts of the gas turbine stage*. PhD thesis, Gliwice, 2012.

[9] *Ansys CFX - Use guide tutorial 9.*.

[10] Dong-Chun C., Rhode D.: *Development of a two-dimensional computational fluid dynamics approach for computing three-dimensional honeycomb labyrinth leakage*. Trans. ASME, **126**(2004), 794–802.

[11] Alizadeh M., Nikkhahi B., Farahani A.S., Fathi A.: *Numerical study on the effect of geometrical parameters on the labyrinth-honeycomb seal performance*. ASME Paper GT2014-25147, 2014.

[12] Snow E.W.: *Diskussionsbeitrag*. Proc. Inst. Mech. Engrs. **166**(1952).

[13] Stocker H.L.: *Determining and Improving Labyrinth Seal Performance in Current and Advanced High Performance Gas Turbines*. AGARDCP-273, 1978.

[14] Zimmermann H., Wolff K.H.: *Air System Correlations Part 1: Labyrinth Seals*. Trans. ASME 1998.

[15] Ansys CFX 16.2 User Guide.